AN ERROR SEPARATION MODEL FOR FORM ERRORS EVALUATION

Fabricio Tadeu Paziani, fpaziani@sc.usp.br
Roberto Hideaki Tsunaki, rtsunaki@sc.usp.br
Benedito Di Giacomo, bgiacomo@sc.usp.br
Departamento de Engenharia Mecânica – Escola de Engenharia de São Carlos – Universidade de São Paulo – Av. Trabalhador Sancarlense, 400 – CEP 13566-590 – São Carlos – SP

Abstract. *The ability to accomplish precise measurements is vitally important to the mechanical industry, where the knowledge of dimensions is essential to guarantee conformity of parts and to control the production processes. The application of automatic systems in tasks formerly made only by the human operator has expanded in the last two decades, to some extent due to the growing market of CNC machines. Such scenario requires the project and construction of automated measuring systems to be integrated to the manufacturing processes. Automatic measuring instruments are especially useful for measurement of large lots of parts aiming at selective assembly and can be faster when compared to conventional techniques. For workpieces that were machined within tight tolerances, automatic measurement offers the advantage of eliminating the influence of the human operator upon measurement. However, automatic equipment always presents reference errors. In order to make measurements independent from reference errors, the application of some error separation technique becomes necessary to allow decoupling artefact errors from those originated in the measuring system. Error separation techniques are especially desired when errors of the measuring system are not negligible when compared to part errors. In these cases, it is wrong to consider the reference given by the instrument. This work presents an automated and dedicated measuring system developed to use a new error separation mathematical model. The measuring system is basically composed of a reference base, a probing device and an error separation mathematical model. Simulations and experimental tests were performed and proved the efficiency of the proposed technique.*

Keywords*: Error Separation, Measurement Automation, Form Error Measurement, Optimization Methods.*

1. INTRODUCTION

One of the main interests of the mechanical industry nowadays is the ability to perform fast and accurate measurements. However, almost all shop-floor measuring processes rely even today on manual instruments and conventional techniques, in spite of the widespread growth of the automatic machines market for the last 25 years. An existing automated manufacturing processes can be enhanced if it is integrated to an also automated measuring system, in the production line. Automatic measuring instruments are especially suited for full-lot inspection aiming selective assembly and interchangeability. Automatic measurement can be quickly achieved if compared to conventional techniques and is free from the influence of the human operator. A relatively simple manner to develop an automated instrument is to utilize an industrial robot as a base.

Industrial robots can easily perform repetitive low-accuracy tasks, such as loading/unloading, welding and painting. Relatively lower initial and lifetime costs, easy programming and fast execution of programmed tasks make robots an attractive investment. However, concerning accuracy requirements, the direct application of industrial robots as measuring instruments is not recommended. Currently available accuracy levels of industrial robot technology, in general, are not enough to allow reliable measurements when taking the robot coordinate system as reference. Factors such as tolerances of robot parts, elasticity at joints, resolvers resolution and control system limitations produce a unique behaviour in each robot, which even limits the application of error compensation techniques.

It should be observed that, in theory, adapting a piece of measuring equipment to the wrist of a robot in order to make measurements will produce results only as accurate as the robot positioning (Greenway, 2000). Therefore, the robot coordinate system cannot be used as a reference. One manner of making measurements independent from robot accuracy is the application of error separation techniques. Then, errors of the artefact can be decoupled from those originated from the robotic measuring system, especially, although not necessarily, when errors from the measuring system are not negligible if compared to measured magnitude. Reversal methods are renowned error separation techniques and are applicable to a wide range of common situations in the mechanical industry. Evans *et al.* (1996) presents a very comprehensive review of various reversal techniques. Compared to reversal, multi-probe error separation techniques present the advantage of avoiding artefact manipulation, although requiring the acquisition of redundant data and besides, depending upon the type of the measured error, a specific probe arrangement is needed. A description of the theory behind both multi-orientation and multi-probe methods can be found in Whitehouse (1976).

Three-probe methods applied to straightness error measurement are allegedly able to separate part error from both translational and angular errors of the scanning stage (Gao and Kiyono, 1996). However, the three-probe method is very sensitive to the presence of zero-adjustment errors of the probes. The difference between the zero-readings of the probes introduces a parabolic error term in the measured profile, which entirely deteriorates the result (Gao *et al.* 2002).

In this work, an innovative error separation model for form errors measurement is presented. The new model is used to decouple form errors of workpieces from errors originated in the measuring system. The latter is basically composed of an industrial robot, specifically arranged displacement sensors and a multi-probe error separation mathematical model. A self-calibration procedure was developed to minimize the influence of zero-adjustment errors between probes. Experimental straightness error measurements were performed and proved the efficiency of the proposed technique.

2. MULTI-PROBE ERROR SEPARATION METHODS

All multi-probe error separation techniques require the manipulation of a chosen degree-of-freedom of the system other than the sensing direction of the sensor. This operation changes the phase of one component of the error (Evans *et al.* 1996). The Three-Probe Method is capable of eliminating the influence of probing system rotational and translational errors, allowing detection of part straightness profile free from the deterioration caused by the measuring system. Figure 1 shows the operational principle of the three-probe method.

Sensor readings *A*, *B* and *C*, represented by S_A, S_B and S_C, can be expressed as a function of system errors at position *i*: Let R_{Pi} be the straightness error of the artefact to be measured, R_{Ri} the probing system translational error motion and δ_i and $-\delta_i$ respective displacement at tips of probes *A* and *C* due to probing device pitch error on the scanning direction. When scanning step is equal to the distance between sensors (L), the three-probe method is referred to as the *S3P* method (*Sequential Three Points*) (Tanaka and Sato, 1986). Otherwise, when scanning step is smaller than L, the three-probe method is referred to as the *G3P* method (*Generalized Three Points*) (Gao and Kiyono, 1997). In the absence of probe calibration errors, both three-point methods allow profile identification from the collected data. In the *S3P* method, sensor readings can be expressed as:

$$\begin{cases} S_{A_i} = R_{P_{i-1}} + R_{R_i} - \delta i \\ S_{B_i} = R_{P_i} + R_{R_i} \\ S_{C_i} = R_{P_{i+1}} + R_{R_i} + \delta i \end{cases} \tag{1}$$

The main error source in the three-probe method consists of the impossibility of providing a global reference for zero-value of all probes, known as zero-adjustment error.

3. AN INNOVATIVE ERROR MODEL FOR STRAIGHTNESS MEASUREMENT

The presence of zero-adjustment errors originates a parabolic error term in the measured profile. In addition, probe position cannot be easily adjusted even with the help of a sufficiently accurate reference flat surface (Gao *et al.* 2002).

Figure 2 shows zero-adjustment errors of sensors in the probing device. Constants k_A, k_B and k_C correspond to the adjustment errors over sensors *A*, *B* and *C* readings, respectively.

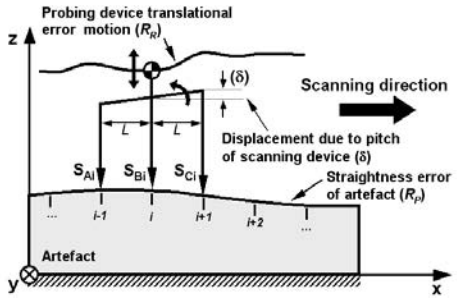

Figure 1. Three-Point Method operational principle

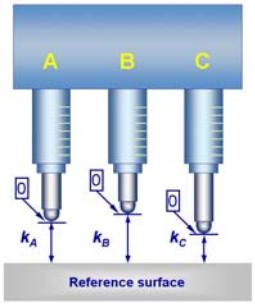

Figure 2. Zero-adjustment errors

The proposed multi-probe method for straightness measurement is described next. As well as the *S3P* method, the proposed technique requires the acquisition of experimental data at steps corresponding to the distance between sensors.

A mathematical model can be developed assuming the hypothesis that four error sources are superimposed at probes output signals: 1) Errors due to workpiece straightness profile; 2) Errors due to probing device translational error motion along the measuring path; 3) Errors due to probing device pitch and 4) Zero-adjustment errors.

Hence, each sensor output signal can be expressed as the superposition of the four already referred error sources:

$$\begin{cases} S_{A_i} = S^P_{A_i} + S^R_{A_i} + S^D_{A_i} + S^E_{A_i} \\ S_{B_i} = S^P_{B_i} + S^R_{B_i} + S^D_{B_i} + S^E_{B_i} \\ S_{C_i} = S^P_{C_i} + S^R_{C_i} + S^D_{C_i} + S^E_{C_i} \quad ,i=1,2,..,N \end{cases} \tag{2}$$

where:

$S_{A_i}, S_{B_i}, S_{C_i}$ are the i^{th} readings of sensors *A*, *B* and *C*, respectively;

$S^P_{A_i}, S^P_{B_i}, S^P_{C_i}$: workpiece straightness errors at the i^{th} measuring point, detected by sensors *A*, *B* and *C*, respectively;

$S^R_{A_i}, S^R_{B_i}, S^R_{C_i}$: industrial robot translational error at the i^{th} measuring point, on sensors *A*, *B* and *C*, respectively;

$S^D_{A_i}, S^D_{B_i}, S^D_{C_i}$: components due to probing device pitch at the i^{th} measuring point, on sensors *A*, *B* and *C*, respectively;

$S^E_{A_i}, S^E_{B_i}, S^E_{C_i}$: components due to zero-adjustment errors at the i^{th} measuring point, on sensors *A*, *B* and *C*, respectively;

i = 1, 2,…, N indicates a measuring point and N is the total number of measurements.

An additional hypothesis, which is implicit in Eq.(2), is that each component can be individually described, i.e., one error source does not alter the behaviour of the others. Consequently, each term of Eq.(2) is independent and can be developed separately. It must be observed that there is no restriction as to relative proportion among contributions.

3.1. Errors due to workpiece profile

The workpiece straightness errors components at the i^{th} measuring point can be written as follows:

$$\begin{cases} S^P_{A_i} = R_{P_{i-1}} + [CA_P + A_P \cdot (i-1)] \\ S^P_{B_i} = R_{P_i} + [CA_P + A_P \cdot (i)] \\ S^P_{C_i} = R_{P_{i+1}} + [CA_P + A_P \cdot (i+1)] \quad i=1,2,\ldots,N \end{cases} \tag{3}$$

where: R_{P_i} is the workpiece straightness error at the i^{th} measuring position and CA_P and A_P are the parameters of the reference line (with relation to a reference system) of the workpiece profile.

3.2. Errors due to robot translational motion along the measuring path

The contribution of the robot translational error motion along the measuring path upon sensor readings can be expressed in the same way as the workpiece profile:

$$\begin{cases} S^R_{A_i} = R_{R_i} + [CA_R + A_R \cdot (i-1)] \\ S^R_{B_i} = R_{R_i} + [CA_R + A_R \cdot (i-1)] \\ S^R_{C_i} = R_{R_i} + [CA_R + A_R \cdot (i-1)] \quad i=1,2,\ldots,N \end{cases} \tag{4}$$

where R_{R_i} is the translational error motion of the industrial robot at the i^{th} measuring position and CA_R and A_R are the robot translational error motion reference line parameters. The translational error motion equally affects all three sensors on a given measuring point, i.e., $S^R_{A_i} = S^R_{B_i} = S^R_{C_i}$.

3.3. Errors due to pitch of probing device along the measuring path

The scanning device pitch error that occurs during the measuring procedure can be expressed as follows:

$$\begin{cases} S^D_{A_i} = -\delta_i \\ S^D_{B_i} = 0 \\ S^D_{C_i} = +\delta_i \quad i=1,2,\ldots,N \end{cases} \tag{5}$$

where δ_i corresponds to the probing device angular error at the i^{th} measuring position, given by:

$$\delta_i = \theta_i \cdot L \tag{6}$$

where θ_i is the probing device pitch error in radians and L is the distance between sensors.

In this case, rotation is supposed to happen around the central sensor. Thus, the angular error produces an increase in $S^D_{A_i}$ and a corresponding decrease of same value in $S^D_{C_i}$, whilst $S^D_{B_i}$ remains unchanged.

3.4. Zero-adjustment errors

The most influential error source on the three-point method is the lack of a single reference for the three sensors. A calibration procedure could be carried out using a reference flat surface in order to align sensors up to a reasonable difference, as shown in Fig. 3(a). However, any minimal discrepancies between the zero values of the three sensors (with relation to an ideal flat surface) produce a large deleterious parabolic error term on the final resulting profile (Gao *et al.* 2002).

The zero-adjustment error can be expressed in several ways, depending on how the reference is chosen. It can be reduced to one adjustment component (calibration constant k_B) on the central sensor if sensors *A* and *C* zero-readings were taken as reference points, as illustrated in Fig. 3(b) Paziani et al. (2007).

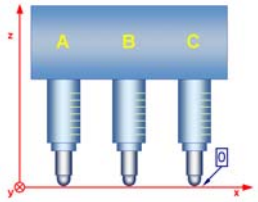

Figure 3 (a). Ideal alignment

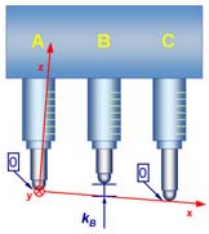

Figure 3 (b). Zero-adjustment error, k_B

The choice of sensors *A* and *C* zero-readings as reference also settles the orientation of a coordinate system. Such orientation is described by two orthogonal axes. *X* axis is defined by the line intercepting the reference points at sensors *A* and *C*, whilst *Z* axis is defined by a line that is normal to axis *X*. The origin of the system coincides with the first point of the workpiece straightness error, which is identically equal to zero as imposed by the model.

Therefore, the contribution due to zero-adjustment errors can be expressed as:

$$\begin{cases} S^{E}_{A_i} = 0 \\ S^{E}_{B_i} = k_B \\ S^{E}_{C_i} = 0 \end{cases} \qquad i = 1,2,..,N \tag{7}$$

where k_B is a constant that describes the zero-adjustment error of the central sensor *B* with relation to a reference system developed from the zero-readings of sensors *A* and *C*. Next, the proposed coordinate system will be used to define the error model. Substituting Eqs.(3), (4), (5) and (7) in Eq. (2) yields:

$$\begin{cases} S_{A_i} = R_{P_{i-1}} + \left[CA_P + A_P \cdot (i-1)\right] + R_{R_i} + \left[CA_R + A_R \cdot (i-1)\right] - \delta_i \\ S_{B_i} = R_{P_i} + \left[CA_P + A_P \cdot i\right] + R_{R_i} + \left[CA_R + A_R \cdot (i-1)\right] + k_B \\ S_{C_i} = R_{P_{i+1}} + \left[CA_P + A_P \cdot (i+1)\right] + R_{R_i} + \left[CA_R + A_R \cdot (i-1)\right] + \delta_i \end{cases} \qquad i = 1,2,..,N \tag{8}$$

Considering a data set of *N* sensor readings, an analysis of Eq.(8) reveals that the system has more unknowns than equations: the number of equations is equal to 3*N*, where *N* is the total number of measured points; the number of unknowns is equal to 3*N*+7, which are detailed below:

R_{P_0} to $R_{P_{N+1}}$ $\rightarrow N$+2 unknowns;

R_{R_1} to R_{R_N} $\rightarrow N$ unknowns;

δ_1 to δ_N $\rightarrow N$ unknowns;

CA_P, A_P, CA_R, A_R and k_B $\rightarrow$ 5 unknowns;

Therefore, the system shown in Eq.(8) is undetermined and it is impossible to find a solution by means of conventional numerical methods. A larger number of equations can be generated either by using more than three sensors or by incorporating experimental data from various runs in a single system. The latter constitutes the proposed methodology, which represents an innovative approach regarding traditional multi-probe error separation methods and is described next.

A mathematical model employing data sets from *M* runs can be derived from the system shown in Eq.(8) simply by generating new equations using additional experimental data sets. The new model will then present *M*(3*N*) equations and *M*(3*N*+7) unknowns, i.e., both number of equations and unknowns were increased by the same amount regarding

the system in Eq.(8). However, it is possible to reduce the number of unknowns assuming that the test conditions remain unaltered during the whole measuring procedure. In other words, the straightness error of the workpiece is considered the same at any run and thus the number of unknowns is reduced by $(M-1)\cdot(N+2)$. Since the experimental data used to increase the number of equations change from run to run, the referred system is made up of linearly independent rows and thus can be solved. The following system is then obtained:

$$
\begin{cases}
S_{A_1}{}^{j} = R_{P_0} + CA_P{}^{h} + R_{R_1}{}^{k} + CA_R{}^{s} - \delta_1{}^{t} \\
S_{A_2}{}^{j} = R_{P_1} + CA_P{}^{h} + A_P{}^{h} + R_{R_2}{}^{k} + CA_R{}^{s} + A_R{}^{s} - \delta_2{}^{t} \\
S_{A_3}{}^{j} = R_{P_2} + CA_P{}^{h} + 2A_P{}^{h} + R_{R3}{}^{k} + CA_R{}^{s} + 2A_R{}^{s} - \delta_3{}^{t} \\
S_{A_4}{}^{j} = R_{P_3} + CA_P{}^{h} + 3A_P{}^{h} + R_{R4}{}^{k} + CA_R{}^{s} + 3A_R{}^{s} - \delta_4{}^{t} \\
\vdots \\
S_{A_N}{}^{j} = R_{P_{N-1}} + CA_P{}^{h} + \left[A_P{}^{h}\cdot(N-1)\right] + R_{RN}{}^{k} + \left[CA_R{}^{s} + A_R{}^{s}(N-1)\right] - \delta_N{}^{t} \\
S_{B_1}{}^{j} = R_{P_1} + CA_P{}^{h} + A_P{}^{h} + R_{R_1}{}^{k} + CA_R{}^{s} + k_B{}^{v} \\
S_{B_2}{}^{j} = R_{P_2} + CA_P{}^{h} + 2A_P{}^{h} + R_{R_2}{}^{k} + CA_R{}^{s} + A_R{}^{s} + k_B{}^{v} \\
S_{B_3}{}^{j} = R_{P_3} + CA_P{}^{h} + 3A_P{}^{h} + R_{R_3}{}^{k} + CA_R{}^{s} + 2A_R{}^{s} + k_B{}^{v} \\
S_{B_4}{}^{j} = R_{P_4} + CA_P{}^{h} + 4A_P{}^{h} + R_{R_4}{}^{k} + CA_R{}^{s} + 3A_R{}^{s} + k_B{}^{v} \\
\vdots \\
S_{B_N}{}^{j} = R_{P_N} + CA_P{}^{h} + \left[A_P{}^{h}\cdot N\right] + R_{R_N}{}^{k} + \left[CA_R{}^{s} + A_R{}^{s}\cdot(N-1)\right] + k_B{}^{v} \\
S_{C_1}{}^{j} = R_{P_2} + CA_P{}^{h} + 2A_P{}^{h} + R_{R_1}{}^{k} + CA_R{}^{s} + \delta_1{}^{t} \\
S_{C_2}{}^{j} = R_{P_3} + CA_P{}^{h} + 3A_P{}^{h} + R_{R_2}{}^{k} + CA_R{}^{s} + A_R{}^{s} + \delta_2{}^{t} \\
S_{C_3}{}^{j} = R_{P_4} + CA_P{}^{h} + 4A_P{}^{h} + R_{R3}{}^{k} + CA_R{}^{s} + 2A_R{}^{s} + \delta_3{}^{t} \\
S_{C_4}{}^{j} = R_{P_5} + CA_P{}^{h} + 5A_P{}^{h} + R_{R4}{}^{k} + CA_R{}^{s} + 3A_R{}^{s} + \delta_4{}^{t} \\
\vdots \\
S_{C_N}{}^{j} = R_{P_{N+1}} + CA_P{}^{h} + \left[A_P{}^{h}\cdot(N+1)\right] + R_{RN}{}^{k} + \left[CA_R{}^{s} + A_R{}^{s}(N-1)\right] + \delta_N{}^{t} \\
j = 1, 2, \ldots, M
\end{cases}
\tag{9}
$$

where:
j designates the run which a given group of equations and respective parameters belong to;
M is the total number of experimental runs;
h is the number of reference lines for the workpiece profile: $h = 0$ or $h = 1$ or $h = M$;
k is the number of measuring system translational error motion sets: $k = 1$ or $k = M$;
s is the number of reference lines for the robot error motion: $s = 0$ or $s = 1$ or $s = M$;
t is the number of scanning device angular error sets: $t = 0$ or $t = 1$ or $t = M$;
v is the number of zero-adjustment errors of the central sensor: $v = 0$ or $v = 1$ or $v = M$.

The system shown in Eq.(9) comprises an adjustable mathematical error model where indices h, k, s, t and v can be appropriately chosen to set the model to meet specific measuring conditions. Considering the determination of only one workpiece profile using data from multiple runs, the system in Eq.(9) becomes overdetermined and therefore can be solved.

The system shown in Eq.(9) can be rewritten in matrix form:

$$\{S\} = [C]\{P\} \tag{10}$$

where $\{S\}$ is a column vector composed by the readings of the three sensors, detailed below;

$$\{S\} = \left[\{S_A\}^1 \{S_B\}^1 \{S_C\}^1 \{S_A\}^2 \{S_B\}^2 \{S_C\}^2 \cdots \{S_A\}^M \{S_B\}^M \{S_C\}^M\right]^T \tag{11}$$

Each element $\{S_A\}^j$ is defined as:

$$\{S_A\}^j = \left[S_{A1}{}^{j}\, S_{A2}{}^{j} \cdots S_{AN}{}^{j}\right] \tag{12}$$

where $S_{Ai}{}^{j}$ is the i^{th} reading of sensor A at the j^{th} run and $\{P\}$ is a column vector composed by the system parameters to be determined (R_P, CA_P, A_P, R_R, CA_R, δ_1, k_B);

$$\{P\} = [\{R_P\}\{CA_P\, A_P\}\{R_R\}\{CA_R\, A_R\}\{\delta\}\{k_B\}]^T \tag{13}$$

where:

$$
\begin{aligned}
&\{R_P\}=\left[R_{P_0}\ R_{P_1}\ R_{P_2}\cdots R_{P_{N+1}}\right]\\
&\{CA_P\ A_P\}=\left[CA_P{}^1\ A_P{}^1\ CA_P{}^2\ A_P{}^2\cdots CA_P{}^h\ A_P{}^h\right]\\
&\{R_R\}=\left[\{R_R\}^1\{R_R\}^2\cdots\{R_R\}^k\right]\\
&\{R_R\}^k=\left[R_{R_1}{}^k\ R_{R_2}{}^k\cdots R_{R_N}{}^k\right]\\
&\{CA_R\ A_R\}=\left[CA_R{}^1\ A_R{}^1\ CA_R{}^2\ A_R{}^2\cdots CA_R{}^s\ A_R{}^s\right]\\
&\{\delta\}=\left[\{\delta\}^1\{\delta\}^2\cdots\{\delta\}^t\right]\\
&\{\delta\}^t=\left[\delta_1^t\ \delta_2^t\cdots\delta_N^t\right]\\
&\{k_B\}=\left[k_B{}^1 k_B{}^2\cdots k_B{}^v\right]
\end{aligned}
\tag{14}
$$

and $[C]$ is the coefficients matrix of parameters $\{P\}$. Matrix $[C]$ is rectangular and defined by the system of Eq.(9).

Once the system in Eq.(10) is developed, a solution is needed for the sought parameters. In this case, however, a traditional solution of the model presents some drawbacks. An analysis of the system reveals that matrix $[C]$ is rectangular, ill-conditioned and rank-deficient. Thus, obtaining a satisfactory solution for the modelled system by means of conventional techniques is not feasible due to the above-mentioned limitations of matrix $[C]$. In this work, the orthogonal-triangular decomposition of matrices (*QR*) is applied to solve Eq.(10). The *QR* decomposition, which is available in MATLAB® package, is appropriate for providing solution for rectangular sparse systems. Supplementary information concerning model building and solution can be found in Paziani (2005) and Di Giacomo *et al.* (2005).

4. THE MEASURING SYSTEM

The Automated and Dedicated Measuring System (ADMSys) is comprised mainly of an ABB IRB140 six-axis articulated industrial robot, which fulfils the application requirements. The control system is provided with analogue-digital conversion circuit board for communication with peripheral equipment.

A especially prepared device for straightness measurement was built to hold three equally spaced LVDT type sensors. The distance between successive sensors is 18 mm, which corresponds to the measuring step. Sensor measuring force is equal to 0.63 N ± 25% and uncertainty is equal to ±1 μm.

Only a minor adjustment of sensors positioning in the probing device is necessary, so that a simultaneously minimal operating range is available to allow measurement. Indeed, fine adjustment is not a requirement, since the remaining zero-adjustment error is included in the previously described mathematical model as a parameter to be calculated.

Sensors were connected to an electronic measuring column for signal conditioning. The measuring column holds up to four sensors and provides independent analogue output signals, which are connected to the A/D acquisition board input channels in a conventional PC.

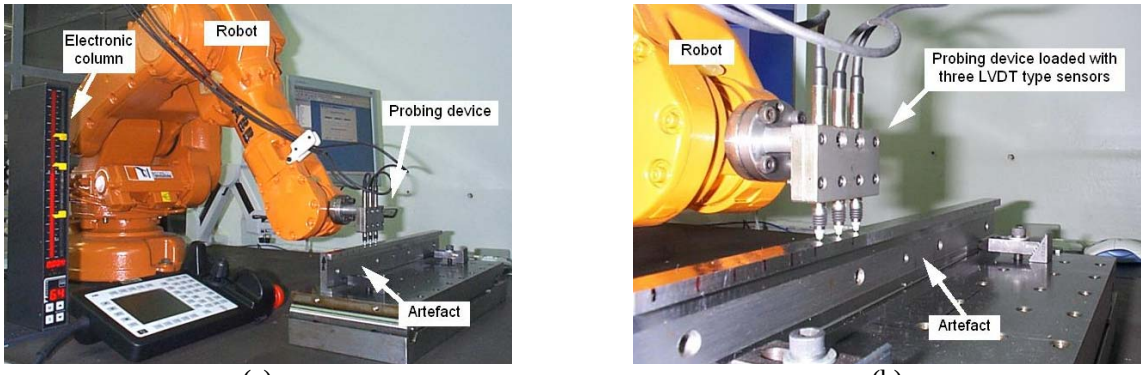

(a) (b)

Fig. 5. The Automated and Dedicated Measuring System (a) and detailed view of probing device (b).

The 12-bit A/D acquisition board presents a total operating range of 600 μm, with resolution of approximately 0.15 μm per A/D level, which is close to the resolution of the sensor itself (0.1 μm, as stated by the manufacturer). In dimensional metrology it is frequently accepted that the repeatability of an instrument corresponds to ten times its resolution. Therefore, the ADMSys is expected to produce satisfactory results at a resolution limit of about 1.5 μm. Considering the influence of other not controlled error sources, such as vibration from the manipulator servomotors

over sensors and the table where the whole system is placed, as well as temperature variation over sensor readings, the system global uncertainty is about 3 μm. In order to provide a more detailed understanding, a theoretical uncertainty analysis is being conduced and hopefully will be soon published.

5. EXPERIMENTAL RESULTS

A laser interferometer system was employed in a series of tests performed to evaluate the robot translational error and probing device pitch error along the measuring path. The results are compared to the ones obtained by the proposed error separation method. The experimental set-up for both measurements is depicted below. Fig. 6 (a) shows the Wollaston prism, as well as the retroreflector and part of the laser head used for measuring the translational error motion of the manipulator. In the same way, Fig. 6 (b) shows pitch measurement with an angular interferometer, an angular reflector, as well as the laser head. Five forward and five backward runs were performed for each measurement.

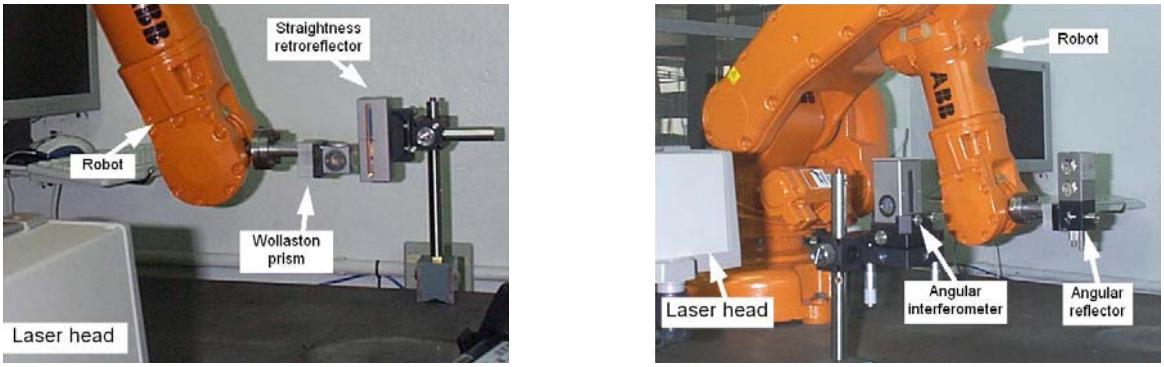

(a) (b)

Fig. 6. Vertical straightness error measurement (a) and pitch error measurement (b).

Figure 7 shows measurement results of the manipulator translational error, R_R. It can be observed that maximum amplitude of the mean forward direction measurement is equal to 99.5 μm ± 5 μm. Also, hysteresis is very pronounced in the range between 100 mm and 250 mm of the measuring length. Such aspects indicate the inadequacy of the manipulator for high positioning accuracy tasks. Had the robot been used as a measuring device without any suitable error separation procedure, only measurements greater than about 1 mm could be obtained.

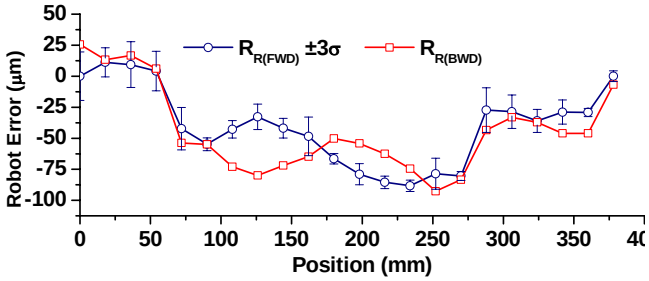

Fig. 7. Robot translation error.

Figure 8 shows the evaluated results of the probing device angular error in the scanning direction. Maximum rotation in the mean forward direction measurement is equal to –96 arcsec, which correspond to an increase of 8.4 μm in sensor *C* reading, as well as a correspondent decrease in sensor *A* reading.

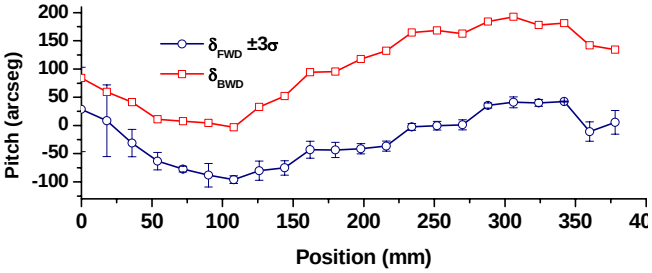

Fig. 8. Pitch error of probing device.

Further experimental tests were carried out to evaluate the proposed system. The straightness errors of both a granite straightedge and a steel artefact were measured using the ADMSys. The steel artefact had been intentionally machined to present pronounced and known straightness errors. The measuring procedure started with the robot activation via analogue to digital (A/D) interface in order to place the probing system at the first measuring point on the artefact. Next, the robot was moved along the artefact longitudinal direction at 18 mm steps and sensor readings were collected at every step. Both artefacts were measured at 23 points along the measuring path and a total of five forward and five backward runs were accomplished.

Since the error separation model is configurable to suit a diverse number of measurement parameters, two different model configurations were employed in this work. The first one, entitled the *Complete Model*, considers that all parameters of Eq.(11) vary from run to run. In other words, the complete model considers that parameters indexed by *h*, *k*, *s*, *t* and *v* of Eq.(11), i.e., are different at each run. Alternatively, in the entitled *Simplified Model*, the parameter given by *h* is considered constant, i.e., the workpiece profile reference line does not vary during the whole measuring process. Next, experimental results from the application of both models are presented.

A Mitutoyo granite straightedge was employed to test the behaviour of the measuring system at its uncertainty limits. First of all, the straightedge was measured by means of the reversal method, which took nearly 30 minutes to be accomplished. The obtained straightness error R_P is equal to 1.5 ± 1.0 μm (2σ). Hence, the straightedge can be taken as a reference for the system, since the accuracy level of the employed industrial robot is much poorer.

Subsequently, the granite straightedge was measured by means of the proposed system. The application of the complete model yielded a straightness error of 3.9 ± 8.8 μm (2σ). Fig. 9 shows the measurement of the granite straightedge using ADMSys complete model.

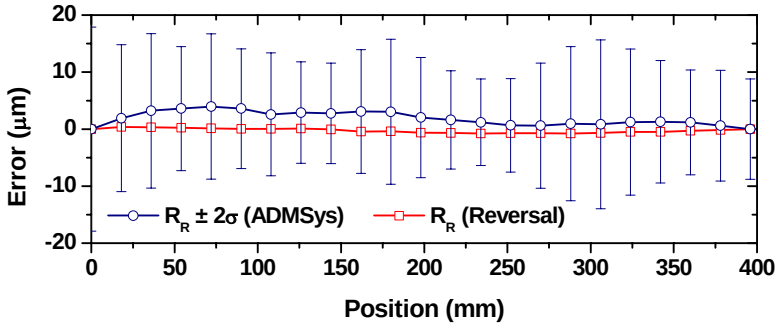

Fig. 9. Straightness error of granite straightedge – Complete Model.

The result using the simplified model produced a straightness error equal to 3.6 ± 8.6 μm (2σ), which is shown in Fig. 10, compared to the reversal. The difference between measurements by ADMSys and reversal can be ascribed to the fact that the measured quantity leans too close to the uncertainty of the proposed system, which is approximately 3 μm. In such situations, the measuring system is prone to error sources that were not considered in the models, as vibration, for instance.

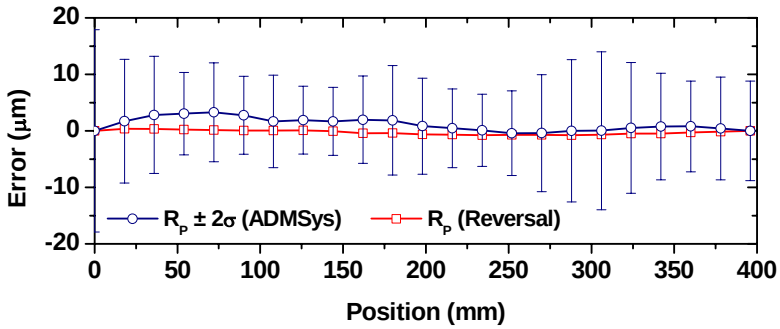

Fig. 10. Straightness error of granite straightedge – Simplified Model.

Fig. 11 shows a comparison between robot translation error decoupled by means of the ADMSys, while measuring the granite straightedge, and the calibration using a laser interferometer. Data was fitted by means of the least squares method. It can be observed that the curves of Fig. 10 present similar behaviour along position axis. Robot translation error measured by the ADMSys is equal to 68.9 ± 5.6 μm (2σ), while the same error measured with a laser interferometer is equal to 76.5 ± 15.2 μm.

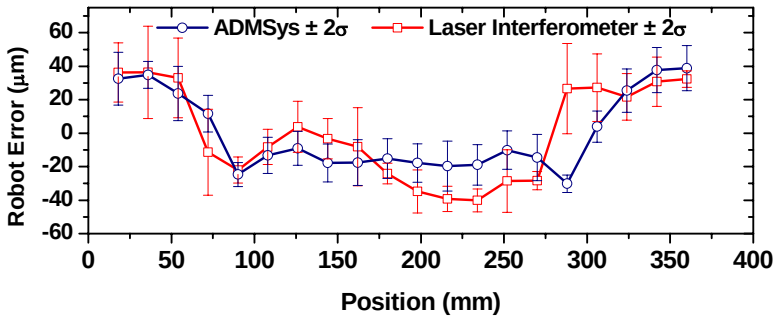

Fig. 11. Robot Translation Error.

The discrepancies, which were rather expected, are a result of the measurement on slightly different lines of action.

Fig. 12 below shows the measurement results of the steel artefact. The straightness error R_P by means of the complete model is equal to 111.4 ± 1.5 µm (2σ), whereas the reversal method yielded 115.9 ± 4.0 µm (2σ). The difference between maximum errors is 4.5 µm, which is equivalent to a percent error of 3.9%.

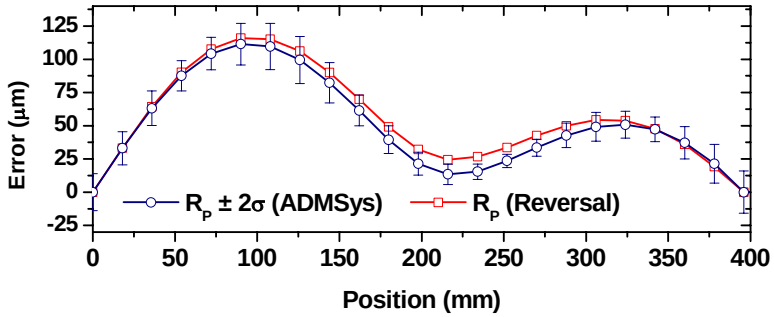

Fig. 12. Straightness error of steel artefact – Complete Model.

In this case, good correspondence between profile shapes can be observed. The improved shape matching may be credited to the fact that steel artefact straightness error magnitude is about the same as robot translational error motion (approximately 100 µm, not shown), allowing better numerical solution of the model.

The results for the application of the simplified method to the steel artefact error are presented next.

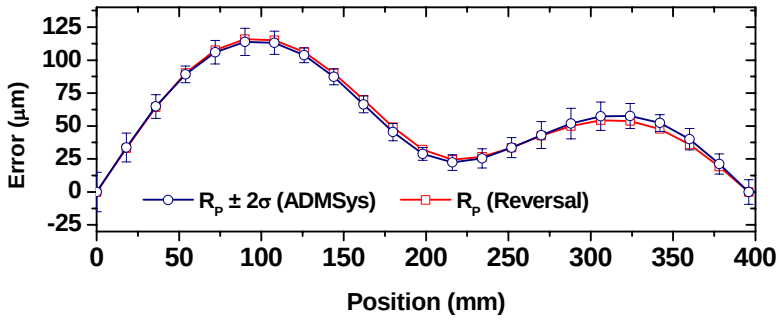

Fig. 13. Straightness error of steel artefact – Simplified Model.

As a result of the application of the simplified measuring model, profile straightness error of the steel artefact, R_P, is equal to 113.9 ± 8.2 µm (2σ), while the reversal method yielded 115.9 ± 4.0 µm (2σ). Percent error between curves of Fig. 13 is equal to 1.7%, which corresponds to less than half the percent error obtained for the steel artefact using the complete model and reveals the adequacy of the adjustable error model to suit different measuring conditions. Average errors are 54.7 µm and 54.9 µm, obtained by the proposed system and reversal method, respectively, which demonstrate good decoupling ability.

6. CONCLUSIONS

A measuring system comprising an industrial robot was developed aiming at the measurement of straightness errors of mechanical parts. The Automated and Dedicated Measuring system (ADMSys) employs as an error separation

technique to decouple part error from errors induced by the measuring system itself. The innovative error model takes into consideration the zero-adjustment errors of the sensors to provide artefacts profile identification in a single operation. The proposed approach also presents low susceptibility to environmental variations and good effectiveness in determining workpiece straightness error.

A probing device was built according to the demands of the error model. Three LVDT type sensors were employed and provided enough resolution to meet most common machining processes accuracy requirements.

An electronic interface was implemented to carry out displacement data acquisition and to make a communication path between the robot control system and a microcomputer in order to activate programmed robot movements. The interface comprises an AD/DA acquisition board, object-oriented software and electric connections.

The error separation algorithm was developed using MATLAB programming environment. The solution for an ill-conditioned linear system of equations was accomplished by means of *QR* decomposition.

Experimental tests were performed both to calibrate the manipulator and to verify the efficiency of the error separation algorithms. Artefacts measurements were completed much faster if compared the reversal method. ADMSys eliminates the influence of the human operator upon results and allows full-lot inspection aiming selective assembly. Finally, the proposed system is mechanical and electronically stable and can possibly be employed at industrial environments

7. ACKNOWLEDGEMENTS

The authors would like to express their gratefulness to Fundação de Amparo à Pesquisa do Estado de São Paulo – FAPESP, and Conselho Nacional de Desenvolvimento Científico e Tecnológico – CNPq, who have been supporting this project.

8. REFERENCES

Di Giacomo, B., Tsunaki, R.H. and Paziani, F.T., 2005, “Robot-based dedicated measuring system with data redundancy for profile inspection”, IEEE/RSJ IROS Int. Conference, Edmonton, Alberta, Canada, pp. 1646-1649.

Evans, C.J., Hocken, R.J., Estler, W.T., 1996, “Self-calibration: reversal, redundancy, error separation, and ‘absolute testing’”, Annals of the CIRP, Vol. 45, No. 2, pp. 617-634.

Gao, W., Kiyono, S., 1996, “High accuracy profile measurement of a machined surface by the combined method”, Measurement, Vol. 19, No. 1, pp. 55-64.

Gao, W., Kiyono, S., 1997, “On-machine profile measurement of machined surface using the combined three-point method”, JSME International Journal, Series C, Vol. 40, No. 2, pp. 253-259.

Gao, W., Yokoyama, J., Kojima, H., Kiyono, S., 2002, “Precision measurement of cylinder straightness using a scanning multi-probe system”, Precision Engineering, Vol. 26, No. 3, pp. 279-288.

Greenway, B., 2000, “Robot accuracy”, Industrial Robot: An international Journal, Vol. 27, No. 4, pp. 257-265.

Paziani, F.T., 2005, “Development of an automated and dedicated measuring system” (In Portuguese), Ph.D. Thesis, Escola de Engenharia de São Carlos, Universidade de São Paulo, São Carlos – SP, Brazil, 2005.

Paziani, F.T., Di Giacomo, B., Tsunaki, R.H., 2007. “Development of an Automated and Dedicated Measuring System for Straightness Evaluation”, J. of the Brazilian Soc. of Mechanical Science and Engineering, Vol. 29 (in press).

Tanaka, H., Sato, H., 1986, “Extensive analysis and development of straightness measurement by sequential-two-points method”, Journal of Engineering for Industry, Vol. 108, No. 3, pp. 176-182.

Whitehouse, D.J., 1976, “Some theoretical aspects of error separation techniques in surface metrology”, Journal of Physics E: Scientific Instruments, Vol. 9, No. 7, pp. 531-536.

5. RESPONSIBILITY NOTICE

The authors are the only responsible for the printed material included in this paper.